2019 IMEKO TC-19 International Workshop on
Metrology for the Sea
Genoa, Italy, October 3-5, 2019

Metrological aspects of the Tombolo effect investigation – Polish case study

Cezary Specht[1], Janusz Mindykowski[2], Paweł Dąbrowski[3], Romuald Masnicki[4], Łukasz Marchel[5], Mariusz Specht[6]

[1,2,3,4,6] *Gdynia Maritime University, Morska 81-87, 81-225 Gdynia, Poland,*
c.specht@wn.umg.edu.pl, j.mindykowski@we.umg.edu.pl, p.dabrowski@wn.umg.edu.pl,
r.masnicki@we.umg.edu.pl, m.specht@wn.umg.edu.pl
[5] *Polish Naval Academy, J. Śmidowicza 69, 81-103 Gdynia, Poland, l.marchel@amw.gdynia.pl*

***Abstract* – Tombolo is a narrow belt connecting the mainland with an island lying near the shore formed as a result of sand and gravel being deposited by sea currents, which is most often created as a result of natural phenomena. However, it can also be caused by human activity, as is the case with the Sopot pier - a town located in the southern part of the Baltic Sea. As a result, the seabed constantly rises and the shoreline moves towards the sea. This paper deals with metrological aspects of the undertaken tombolo effect investigation, namely accuracy analysis of the measurement results. Aforementioned analysis concerns two methods used for creating a 3D beach model: firstly using images from unmanned aerial vehicles (UAV) and secondly, based on geodetic laser scanning (TLS – Trimble Laser Scanner).**

I. INTRODUCTION: TOMBOLO EFFECT – POLISH CASE STUDY

Sopot is one of the major Polish holiday and spa resorts situated on the Baltic Sea coast. The city has the longest wooden pier in Europe, which is regularly damaged by storms. In October 2009, a violent storm completely destroyed the wooden structure of the pier groyne. The only economically viable method for protecting the pier was to build two breakwaters from the southern and eastern sides. The waterbody bordered between these breakwaters and the pier groyne and head has become a natural marina. In 2010, expert discussions and their opinions resulted in a decision to build a yacht marina in Sopot (3 basins, a maximum of 103 vessels: 40 large ones up to 14 m in length, and 63 smaller ones up to 10 m in length) for 72 million PLN. The seemingly undoubted decision is currently becoming a serious problem for the city, as the construction of the marina led to the local stoppage of the sand transport along the coast, which resulted in its accumulation between the marina and the shore and the shift of the coastline towards the sea (approx. 50 m), and initiated the process of the inevitable formation of a peninsula in Sopot. Such an oceanographic phenomenon known as tombolo [1] is most frequently influenced by the course of beaches and coasts under natural conditions but can also result from human activities, as is the case in Sopot [2]. In the Bay of Gdańsk, the strongest surface wind waving is generated from direction N towards E. The waves that reach the beach in Sopot from the E direction hit diagonally against the shore and cause the movement of bottom sediments along the coast. After the marina was built, its breakwater significantly decreased the wave energy, moreover, waves are deflected at its ends (Fig. 1), which results in the formation of two vortexes (directed opposite to each other). Consequently, the seafloor between the marina (obstacle) and the shore is elevated upwards, which results in the development of a morphological formation known as a tombolo. It should be stressed that this phenomenon in Sopot is unique in Poland.

Following this chapter, the rest of the article is structured in this way: Section II shortly describes methodology of geodetic and hydrographic measurement used for the studied area of the shore and the seabed, Section III presents basic information about applied algorithms and metrological parameters of the related measurement instrumentation and Section IV, fundamental for this paper is devoted to the accuracy analysis of the measurement results. The last section is a conclusion of the study.

Fig. 1. The nature of the phenomenon that causes the formation of the tombolo effect (on the left), and the wavy surface of the sea in varying directions resulting from the diffraction of waves the marina breakwater in Sopot (on the right).

II. METHODOLOGY OF GEODETIC AND HYDROGRAPHIC MEASUREMENTS TO ILLUSTRATE THE STUDIED AREA OF THE SHORE AND THE SEABED

In order to conduct the proposed study, the team of researches intends to apply and integrate, in measurement terms, two technical solutions whose development began as late as in the second decade of the 21st century, i.e. unmanned aerial vehicles (UAV) [3] and unmanned surface vehicles (USV) [4,5]. They will enable the investigation of the tombolo phenomenon in Sopot in two basic geospatial aspects:

1. Photogrammetric – designed to assess changes in the beach surface relief and the coastline course based on 3D land modelling using photogrammetric methods (UAV) [6]. The analysis of the phenomenon covers an 800 x 200 m area (beach).
2. Hydrographic – aimed at determining the seafloor relief, the amount of material (sand) accumulated in the vicinity of the pier and the marina and the level of increase in its volume as a function of time. To this end, acoustic sounding for the waterbody with the dimensions of 800 x 400 m should be regularly carried out. In view of the depths (of less than 1 m) prevailing in this region, it is recommended that a hydrographic unmanned surface vehicle be used [2].

During measurements USV used two independent positioning systems. The first system consisting of low-cost multi-GNSS receiver (u-blox NEO-M8N) with a built-in Fluxgate was used to control the hydrographic unit course in automatic mode, using the PixHawk Cube autopilot. According to the instructions, the accuracy of determining the position of this device is 3-5 m ($p = 0.95$). The second positioning system was the Trimble R-10 geodetic receiver, working in real time, using the Real Time Satellite Geodetic Network - VRSNet ensuring horizontal accuracy of position determination at the level of 3-5 cm ($p = 0.95$) [7]. This is the typical accuracy of the majority of such networks working in the world. This receiver was connected to a single beam echo sounder SonarMite BTX (SBES).

Creating a 3D beach model can be done on the basis of two methods: using images from unmanned aerial vehicles or make measurements based on geodetic laser scanning [8].

In view of the elongated surface nature of the beach under measurement, it was necessary to plan and arrange an appropriate number of sites. The measurement was taken with a Trimble TX8 laser scanner without the photo-taking option. Hence, the obtained point clouds had only colours resulting from the calculated laser beam reflection intensity. To cover the assumed study area, it was necessary to establish 27 sites located at a distance of approx. 60 m from each other (Fig. 2). In view of the small number of characteristic objects to be used for the recording of a point cloud in the field at a later time, spherical tags located in the sand in a manner ensuring the stability of their position were used. The tags had to be located a relatively short distance from the neighbouring measurement sites; therefore, they were located halfway between them or in their immediate vicinity. Such an approach ensured that a relatively large set of points on the spherical tag's surface were obtained during the measurement. This enabled the precise fitting of spheres into the set of points and the determination of their midpoints which, in the recording process, were the points of adjustment of particular local point cloud systems.

Fig. 2. TLS – the location of laser scanner measurement sites.

Photogrammetric flight pass was performed using a DJI Mavic Pro drone independently for each of the adopted parts. The data were recorded using a Pix4D Capture mobile application. During the mission, 621 photographs were taken at an altitude of 60 m above the drone take-off level (the beach). The obtained average GSD coefficient value amounted to 2.25 cm/pix at a camera resolution of 4000 x 3000 effective pixels. The overlap parameter defining the degree of photograph overlapping in transverse and longitudinal directions was determined to be 80%. The main parameters of the camera are: Sensor: 1/2.3" (CMOS), effective pixels -12.35 M (total pixels: 12.71 M); Lens: FOV 78.8° 28 mm (35 mm format equivalent) f/2.2; Distortion: < 1.5% focus from 0.5 m to ∞ .

A photogrammetric model was developed using the Pix4d Mapper Pro software which enables photographic data processing and generating based on three-dimensional models and orthophotomaps. A median of 21,128 nodal points on a single photograph was obtained, which indicates a relatively high number of characteristic points and areas, considering the frequently little diversified coverage of the area surface. A camparative picture of point clouds is illustrated in Figure 3, obtained from measurements using TLS and UAV methods.

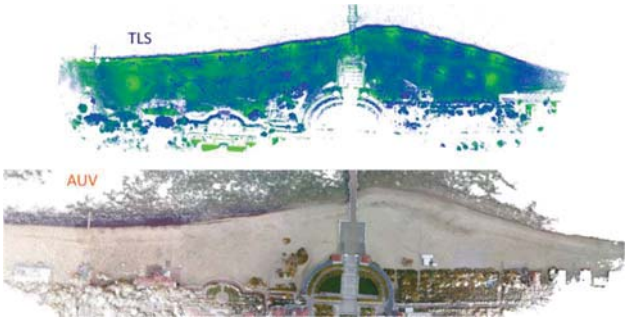

Fig. 3. TLS and UAV – point clouds originating from the measurement using two methods.

III. APPLIED ALGORITHMS AND METROLOGICAL PROPERTIES OF THE RELATED MEASUREMENT INSTRUMENTATION

Applied laser scanning method concerns the measurement of coordinates X-Y-Z of the investigated terrain points. This method is reffered to here as TLS method because the measurement was taken with a Trimble Tx8 laser scanner. This method shows a very good accordance of measurement results with mandatory system of geographic coordinates. Measurement results obtained in the local system are transferred to PL-2000 national system. Accuracy of the final data results depends only from the laser instrumental accuracy and accuracy of the reference points localization, that is, the points, which were used to transformation into PL-2000 system (Fig. 4).

Fig. 4. Algorithm of the TLS method accuracy estimation, where: Δ_{Tx8}, $\Delta_{PL-2000}$ – absolute errors corresponding the Trimble Tx8 laser scanner and PL-2000 national system, respectively, u_{TLS} – uncertainty of the considered method.

In the discussed TLS case study, the detailed inaccuracy components of the applied laser scanner measurement are equal to:

- inaccuracy of laser Trimble Tx8 – 1 cm horizontally and 1,5 cm vertically,
- inaccuracy of satellite receiver R10 used to determine the coordinates of reference points – 1 cm horizontally and 1,5 cm vertically,
- inaccuracy of the PL-2000 system – 2 cm horizontally and vertically.

A cloud of TLS points after transformation to PL-2000 system, including the data collected at the determined area (terrain), can be a reference set for cloud of points obtained by use of the UAV method in the form of terrain digital photos. A series of photos, processed by the adequate program, enables to create a space projection of the investigated area (terrain), in which beside of X-Y coordinates the Z coordinate is determined in relation to each point of the cloud. On the basis of the reference points coordinates, the obtained local coordinates are transformed into PL-2000 system. In practice, the sequence of operations realized on the basis of photo-data does not allow to achieve a satisfactory level of accuracy of the data on the investigated area.

In the UAV method of terrain imaging, the picture processing operation resulted in the generation of a cloud containing 20,666,253 points, which translates into a density of approx. 117 points per m^2. Numerical data processing was carried out using a high-parameter workstation (16 GB RAM, i7-6600U, GTX 1070) and lasted for 3 hours 42 minutes. The following values of errors for particular coordinates were obtained: 2.83 m (X), 4.08 m (Y) and 9.81 m (Z).

In the discussed UAV case study the detailed inaccuracy components of the applied unmanned aerial vehicle are equal to:

- camera pixel resolution – 2,25 cm,
- inaccuracy of UAV position: X, Y – a few meters, Z – several meters.

To estimate the quality of the UAV method measurement, it is proposed to use the TLS data cloud as reference data. These data are obtained in the same area as the data in the UAV data cloud. Then, it is possible to estimate the systematic X-Y-Z coordinates errors components in the UAV cloud, as well as their dispersion (noise) in relation to reference values (Fig. 5).

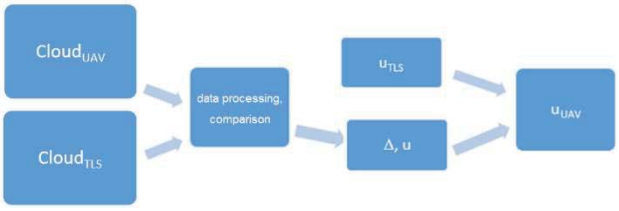

Fig. 5. Algorithm of the UAV method accuracy estimation, where: $Cloud_{UAV}$, $Cloud_{TLS}$ – clouds of points related to the methods UAV and TLS, respectively, Δ, u – absolute values of occurred errors and related uncertainties, u_{TLS}, u_{UAV} – measurements uncertainties characterizing the methods TLS and UAV, respectively.

Dedicated software is currently under construction to allow for the determination of the uncertainty characteristics of X-Y-Z coordinates collected in large data files obtained using the UAV method.

IV. ACCURACY ANALYSIS OF THE MEASUREMENT RESULTS

Results of the executed measurements of the terrain geometry are treated as random variables, that is they are subject to statistical rules and the probability calculus is used to assess them. The term “Metrological aspects” in this paper concerns the estimation of uncertainty in

relation to the carried out measurements of the shore and the seabed under investigation. Measurement results obtained with use of the aforementioned methods defined as TLS and UAV, respectively, create the series (clouds) of measurement points. Each of them has different reference in the X-Y-Z coordinates system. In consequence, it is possible to estimate an uncertainty of determination of space coordinates of each measurement point in cloud with applying the methodology of type B uncertainty determining [9]. Uncertainty of type B concerns mainly the estimation of inaccuracy of measurement instrumentation. Its calculation requires of absolute error threshold value ΔX_t determining and assumption of the given function of probability distribution for this error. Then, for a given component, the type B extended uncertainty $u_B(x)$ is expressed as:

$$u_B(x) = \frac{\Delta X_t}{3} \quad (1)$$

- for normal distribution or

$$u_B(x) = \frac{\Delta X_t}{\sqrt{3}} \quad (2)$$

- for uniform distribution,

where: ΔX_t – maximum permissible error threshold value, $u_s(x)$ – standardized, simple uncertainty.

Taking into account the measurement parameters characterizing the measurement instrumentation used in described experiments (section III) we can calculate complex uncertainty $u_c(x)$ as:

$$u_C(x) = \sqrt{u_{B1}^2(x) + u_{B2}^2(x) + \cdots u_{Bn}^2(x)} \quad (3)$$

where: $u_{B1(x)}$, $u_{B2(x)}$ … correspond to all sources of errors in the considered measurement procedure.

Then, for a given component, the type B extended uncertainty $U_B(x)$ is expressed as:

$$U_B(x) = k \cdot u_c(x) \quad (4)$$

where: k – coefficient of extension (coverage factor).

First of all, the detailed uncertainty components can be analysed and calculated for the method TLS and related to it measurement instrumentation. Taking into consideration known instrumental and method data, the following error components are considered:

- reference system TLS accuracy,
- satellite receiver R10 maximum errors,
- PL-2000 system errors threshold values.

The uncertainty should be estimated for all three coordinates (X, Y and Z). The uncertainty budget is shown in Table 1 for X or Y coordinates and in Table 2 for Z coordinate.

Table 1. Uncertainty budget (X or Y coordinate) of TLS system.

Quantity	Maximum error	Probability distribution	Standard uncertainty
$(X,Y)_{Tx8}$	1 cm	uniform (2)	0.58 cm
$(X,Y)_{R10}$	1 cm	uniform (2)	0.58 cm
$(X,Y)_{PL-2000}$	2 cm	uniform (2)	1.15 cm
$u_{TLS}(X,Y)$			1.41 cm

Table 2. Uncertainty budget (Z coordinate) of TLS system.

Quantity	Maximum error	Probability distribution	Standard uncertainty
$(Z)_{Tx8}$	1.5 cm	uniform (2)	0.87 cm
$(Z)_{R10}$	1.5 cm	uniform (2)	0.87 cm
$(Z)_{PL-2000}$	2 cm	uniform (2)	1.15 cm
$u_{TLS}(Z)$			1.68 cm

Assuming the normal distribution of complex uncertainties for all coordinates, the expanded uncertainty (4) U_{TLS} is 2.42 cm (X or Y coordinate) and 3.36 cm (Z coordinate) (p=95 %).

V. FINAL REMARKS

The coastline around the pier in Sopot is constantly changing. This is done mainly as a result of the construction of an additional breakwater protecting the pier against storms. It is therefore necessary to conduct continuous cartographic monitoring in this area.

The article presents the methodology for conducting this monitoring and the methodology for assessing its accuracy.

The UAV method (images) is less accurate, but allows the Digital Terrain Model to be made in a relatively short time and with the use of inexpensive equipment. However, the TLS method (laser scanning) is time-consuming, precise and requires expensive equipment. For this reason, the aim of the paper is to assess the accuracy and effectiveness both methods under real, terrestorial conditions.

Future works will be focused on carying out in-depth comparative accuracy analysis of creating a 3D beach model using photogrammetric measurements (derived from UAV), when adopted as a reference model derived from measurements using a laser scanner. The point cloud obtained from the TLS method can be used to assess the accuracy of the UAV method and to correct the systematic errors that accompany it. Software being developed for UAV measurement accuracy assessment performs the data analysis in several steps programmed in the algorithm implementing:

- organizing point clouds: sorting by coordinates,
- random noise filtering,
- determining standard deviation within selected areas,
- determining systematic interactions by comparing UAV and TLS data,
- correction of point coordinates,
- presenting the results of the assessment and their analysis.

REFERENCES

[1] Mohamed A.S., “2D and 1D Numerical Model Simulations for the Effect of a Single Detached Breakwater on the Shore”, MSc Thesis, Delft

University of Technology, Delft, 1997.
[2] IO PAN, “Wykonanie badań i prac modelowych dna i brzegu morskiego w okolicy mola w Sopocie”, 2016, bip.umsopot.nv.pl/Download/get/id.32756.html [09.06.2019].
[3] Fritz A., Kattenborn T., Koch B., “UAV-Based Photogrammetric Point Clouds – Tree Stem Mapping in Open Stands in Comparison to Terrestrial Laser Scanner Point Clouds”, International Archives of the Photogrammetry, Remote Sensing and Spatial Information Sciences, Vol. XL-1/W2, 2013, pp. 141-146.
[4] Stateczny A., Grońska D., Motyl W., “Hydrodron – New Step for Professional Hydrography for Restricted Waters”, Proceedings of the 2018 Baltic Geodetic Congress (Gdańsk, Poland), 2018, pp. 226-230.
[5] Specht C., Specht M., Cywiński P., Skóra M., Marchel Ł., Szychowski P., “A New Method for Determining the Territorial Sea Baseline Using an Unmanned”, Hydrographic Surface Vessel, Journal of Coastal Research, 2019, pp. 1-12.
[6] Baptista P., Bastos L., Bernardes C., Cunha T., Dias J., “Monitoring Sandy Shores Morphologies by DGPS – A Practical Tool to Generate Digital Elevation Models”, Journal of Coastal Research, Vol. 24(6), 2008, pp. 1516-1528.
[7] Specht C., Specht M., Dąbrowski P., 2017, “Comparative Analysis of Active Geodetic Networks in Poland”, 17th International Multidisciplinary Scientific GeoConference SGEM Conference Proceedings, Vol. 17, Issue 22, 29 June - 5 July, Albena, Bulgaria, 2017, pp. 163-176.
[8] Ruggles S., Clark J., Franke K.W., Wolfe D., Reimschiissel B., Martin R.A., Okeson T.J., Hedengren J.D., “Comparison of SfM Computer Vision Point Clouds of a Landslide Derived from Multiple Small UAV Platforms and Sensors to a TLS based Model”, Journal of Unmanned Vehicle Systems, Vol. 4(4), 2016, pp. 246-265.
[9] “Evaluation of measurement data – Guide to the Expression of Uncertainty in Measurement”, (GUM 1995 with minor corrections), JCGM (Joint Committee for Guides in Metrology), 2010